SCIENCE AND INNOVATION
INTERNATIONAL SCIENTIFIC JOURNAL VOLUME 2 ISSUE 6 JUNE 2023
UIF-2022: 8.2 | ISSN: 2181-3337 | SCIENTISTS.UZ

SYNTHESIS OF $SiO_2 \cdot xZrO_2$ NANOPOROUS SORBENTS AND THEIR TEXTURE AND SORPTION CHARACTERISTICS

[1]Uzokov Javlon Rustamboyevich, [2]Muxamadiyev Nurali Qurbonaliyevich, [3] Turayev Begzod Gulomovich, [4] Kungratov Kamoliddin

[1,2]Samarkand State University, Samarkand, Uzbekistan

[3,4]Academic lyceum under Samarkand State University

https://doi.org/10.5281/zenodo.8020839

Abstract. *Composite sorbents containing $SiO_2 \cdot xZrO_2$ (x=0,3; 0,5; 0,7) were synthesized using sol-gel technology in different solution media and temperatures. The effect of quantitative ratios of reagents, solution medium and temperature on texture characteristics of the sorbents: the specific surface area, the formation of pores, the size and the average diameter were studied. The texture and sorption characteristics of the sorbents were studied by adsorption of benzene, hexane, and toluene vapors in a McBen-Bakra vacuum device. According to it, the specific surface area of the sorbents prepared at 30°C (S_{BET}, m^2/g) is 710,3÷975,6 m^2/g, the average diameter of the pores is 0,8÷2,5 nm, the specific volume of the pores (V_s cm^3/g) was found to be equal to 0,155÷0,309 cm^3/g. In the sorbents synthesized at 50°C, 70°C and 90°C, the specific surface area was found to be 350,6 ÷ 870,9 m^2/g, and the average diameter of the pores was 2,8÷72,8 nm. The phase composition of the sorbents was studied by X-ray diffractometry (XRD), the surface morphology by scanning electron microscopy, and the element composition by X-ray microanalysis.*

Keywords: *sol-gel technology, nanocomposite, sorption isotherm, average diameter of pores, specific surface area.*

Graphical Abstract

Schematic representation of the synthesis of $SiO_2 \cdot xZrO_2$ nanocomposite

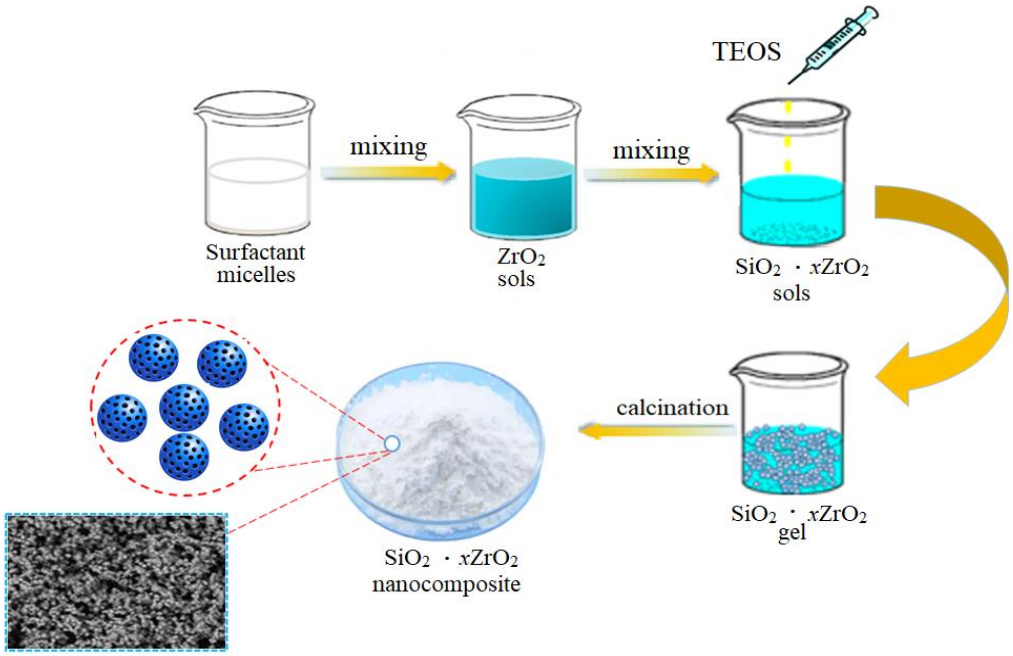

Highlights:

- Composite sorbents containing $SiO_2 \cdot xZrO_2$ (x=0,3; 0,5; 0,7) were synthesized using sol-

gel technology.

- The specific surface area (S_{BET}, m^2/g) of the sorbents prepared at 30°C was found to be 975,6 m^2/g, and that of the sorbents prepared at 120°C was 350,6 m^2/g.
- The sorption capacity of benzene vapors in the sorbents synthesized at 30°C was found to be 6,2 ± 0,08 mol/kg.

1.Introduction

In the last twenty years, the synthesis of nanomaterials with different physicochemical properties has increased dramatically [1]. In the synthesis of this type of material, unique hybrid nanocomposites were prepared based on the introduction of various functional group monomers, polymers, oxides of variable valence metals into the reaction system and on mathematical modeling of the reaction process [2-8]. Among the nanomaterials, micro and mesoporous silica and composite materials based on it are of special importance and their application is due to the size of pores in the nanometer range, the specific surface area, porosity, high sorption and catalytic activity [9-13].

The role of porous nanomaterials in the production of thermal insulation coatings, alternative energy, as a catalyst, in the creation of chemical sensors, as a medicine carrier (nanocontainer), in gene isolation, as a binder of some viruses, in immobilization of enzymes, in solving environmental problems and in electronics is invaluable [14-23].

In the synthesis of mesoporous sorbent, the formation of their textural properties, namely the specific surface of sorbents (S_{BET}, m^2/g), the specific volume of pores (V_s, cm^3/g) and the average diameter of pores (D, nm) are directly affected by the solution medium, the temperature, the type of surface active substances, the hydrolysis catalyst and the quantitative ratio of reagents. In the synthesis process studying the influence mechanism of these factors allows to manage the formation of porous dimensions of the sorbent synthesized and to carry out targeted synthesis [24].

Kao and his colleagues [25] studied in detail the effects of the quantitative ratios of reagents $H_2O/Si(OC_2H_5)_4$ on the pores size of the sorbents prepared. It was found that, when the ratio of $H_2O/Si(OC_2H_5)_4$ is 8:4 the xerogels formed composed of micropores. While the ratio of $H_2O/Si(OC_2H_5)_4$ was 10:1, the induction period of the gelation process was short, and forming micropores of the xerogels was accelerated. The formation of xerogels consisting of branched orderly mesopores was observed when the quantitative ratio of $H_2O/Si(OC_2H_5)_4$ was 4:1.

The hydrolysis reaction of silicon alkoxides is carried out under acid or alkaline conditions. In the condition, where the pH is neutral, the value of the hydrolysis degree is determined to be the smallest [26]. Ying and Benziger [27] studied the effect of the solution medium on the rate of the reactions of hydrolysis and polycondensation, as well as on gel formation in the synthesis of mesoporous nanomaterials. They observed the change in the interaction of TEOS with cation surfactants in different pH value of a solution, as well as a sharp change in the particles size in the mesoporous nanomaterials formed in the synthesis process. For example, they observed that at the isoelectric point (pH=2.0) the condensation reaction would go slowly due to weak interaction of the primary colloidal particles formed from the hydrolysis of TEOS with the molecules of the cation surface active substance, while at pH=6,0-9,0 the formation of mesoporous silica nanoclasters accelerated [28].

The interaction of silicon and metal alkoxides with the surface active substances of this type consists of S^+I^-, $S^+X^-I^+$, S^-I^+, $S^-X^+I^-$, $S^0X^+I^-$, S^0I^0, $S^0H^+X^-I^+$ (S-type of a surface active substance, I-silicon alkoxide, X-inorganic salts). In sol-gel process the positive charge density is

high in pH value of 2, to say that in the isoelectric point. This slows the formation of a bond between the correct micella and silanol Si-OH groups formed by the cation surface active substance. Therefore, a sorbent with irregular pores is prepared from the gel formed in this order. The density of the negative charge in the solution increases at pH=6.0÷10.0. In this case, since the formation of the bond between the correct micella and silanol groups formed from the cation surface active substance is positive the gel prepared allows to synthesize a sorbent consisting of ordered pores of the same size [29].

The authors [30] mixed TEOS and water in the proportion of 1:4 moles and prepared a porous silica gel at different temperatures by the methods of simple hydrothermic and microwave heating without any additives. By checking the samples prepared by both methods, it was determined that the size of the specific surface area of the samples by BET decreases with the increase in the temperature. The researchers concluded that this is due to an increase in the rate of condensation reaction at high temperatures.

The authors [31] determined a decrease in the density of silica prepared at 54°C and 70°C from 1,46 g/cm^3 to 0,98 g/cm^3. But the researchers did not give an explanation for the decrease in the density of silica gel with an increase in temperature.

Khodaee and colleagues [32] observed the change in particle size 84-115 nm, 86-94 nm and 135-160 nm respectively with an increase in temperature in porous silica samples prepared from TEOS, ethanol and CTABr as surfactant at 30°C, 50°C and 80°C using the sol-gel technology.

Gupta and his team has synthesized the ionic gels containing mesoporous silica matrix in ionic liquid at different temperatures using the anhydrous sol-gel technology. The researchers synthesized the mesoporous silica nanomaterials using 1-ethyl-tetrafluoroborate 3-methylimidazole and TEOS as SiO_2 source, formic acid as a catalyst at temperatures of 0°C, 30°C and 210°C. They studied the effect of the temperature on the degree of gelation, the density of ionogels and pores parameters [33].

The sol-gel technology is the most effective approach to the preparation of porous nanomaterials. The method is characterized by simplicity of equipments, cost effective, environmental safety, low cost of the product [34-35]. The sol-gel technology is also characterized by the soft hydrolytic polycondensation reaction of primary precursors and the opportunity to add monomers, polymers, oxides of variable valence metals with functional group to the reaction system, the use of a single solvent for all reagents and the control of the structure and size of the final product.

2.Experimental

2.1 Materials and methods

TEOS-$(C_2H_5O)_4Si$ was used as a source of SiO_2 in the synthesis of $SiO_2 \cdot xZrO_2$ composite sorbents (Jinan Xinggao Chemical Technology Co., Ltd, China, purity> 98.6%), zirconium (IV) oxynitrate dihydrate $ZrO(NO_3)_2 \cdot 2H_2O$ (purified by recrystallization >99.6%) for preparation of ZrO_2 sols. Double distilled ethyl alcohol (purity> 96,2%) was used as solvent. To study the effect of a catalyst and solution medium on the texture characteristics of the sorbents, the solutions of 1 M HCl (pH =2,0), 0,1 M CH_3COOH ($K_\partial = 1,8 \cdot 10^{-5}$, pH=5,2) and 0,01 M NH_4OH ($K_d = 1,76 \cdot 10^{-5}$, pH=10,3) were used. During the synthesis, the solution medium was monitored using a Mettler Toledo FP-20 pH meter. To study the effect of the temperature on the formation of specific surface area (S_{BET}, m^2/g), pore size (V, cm^3/g) and average diameter (D, nm) of the sorbents, the synthesis

was carried out at 30°C, 50°C, 70°C, 90°C, 120°C. The texture characteristics of the sorbents were studied by adsorption of benzene, toluene, and hexane vapors using McBen-Bakra sensitive quartz spiral device [40]. The surface morphology and porosity of the nanocomposite sorbents were studied by scanning electron microcopy using SEM EVO MA 10 (Carl Zeiss, Germany) scanning electron microscope. The elemental analysis of the sorbents was performed using a detector (EDS Aztec Energya Adyanted X-Act, Oxford Instruments) attached to the scanning electron microscope SEM EVO MA10 (Carl Zeiss, Germany).

2.2 Synthesis of $SiO_2 \cdot xZrO_2$ composite sorbents

The $SiO_2 \cdot xZrO_2$ nanocomposite sorbent samples were synthesized in the following sequence:

1. In a dilotometer placed in a magnetic stirrer 10 ml of the solution of containing 0.003 mol (1 g) cetyltrimethylammonium chloride ($C_{19}H_{42}ClN$) was added to 100 ml of water-alcohol mixture. Then was added 5ml of 0,01 M solution of NH_4OH (1M solution of HCl for acidic medium) was added to the solution. 2. The following amounts of $ZrO(NO_3)_2 \cdot 2H_2O$ crystal hydrate were used to prepare samples of $SiO_2 \cdot xZrO_2$ (0,3÷0,7) nanocomposite sorbents. 1,602 g (0,006 mol) $ZrO(NO_3)_2 \cdot 2H_2O$ crystal hydrate was dissolved in the solution prepared for $SiO_2 \cdot 0{,}3ZrO_2$, 2,670 g (0,01 mol) crystal hydrate for $SiO_2 \cdot 0{,}5ZrO_2$ and 3,738 g (0,014 mol) crystal hydrate for $SiO_2 \cdot 0{,}7ZrO_2$ sorbent synthesis. 3. 10 ml of an alcoholic solution containing 4.16 grams of TEOS was then added dropwise to the solution for 30 minutes. 4. The resulting colloidal solution was placed in a thermostat and stirred at a constant temperature for 24 hours, until a gel was formed. 5. The resulting gel was washed several times with distilled water. 6. The samples were dried at 105°C for 4 h. 7. The samples of porous $SiO_2 \cdot xZrO_2$ nanocomposite sorbents were prepared by calcining the dried powder in a furnace (Witeg, GmbH. Germany) at 500°C for 8 hours (calcination stage).

3. Results and discussion

In the synthesis of $SiO_2 \cdot xZrO_2$ nanocomposite sorbents using sol-gel technology, an increase in the concentration of ZrO_2 sols in solution leads to a change in their specific surface area (S_{BET}, m^2/g), pore size (V, cm^3/g) and average diameter (D, nm). When the solutions of ZrO_2 sols with the concentration of 0,03; 0,05; 0,07 at 50°C is used the texture characteristics have been changed in the order given in table 1.

Table 1

Texture characteristics of sorbents $SiO_2 \cdot xZrO_2$ (x = 0,3; 0,5; 0,7)

C_M (mol /l)	S_{BET}, m^2/g	V, cm^3/g	D, nm	ρ, cm^3/g
0,03	975,6±92,6	0,82±0,09	6,5±0,5	0,34±0,06
0,05	768,4±78,4	0,65±0,06	52,4±3,8	0,73±0,06
0,07	302,6±35,8	0,34±0,04	60,2±4,6	0,95±0,10

It was found that the specific surface area of the sorbent $SiO_2 \cdot 0{,}3ZrO_2$ is 1,27 times larger than the specific surface area of the sorbent $SiO_2 \cdot 0{,}5ZrO_2$, and 3,22 times larger than the surface area of the sorbent $SiO_2 \cdot 0{,}7ZrO_2$. An increase in the average diameter of the pores was observed with an increase in the amount of ZrO_2 in the sorbent samples $SiO_2 \cdot xZrO_2$. It was also found that with increasing content of ZrO2 in the composite sorbent $SiO_2 \cdot xZrO_2$ (0,3÷0,7), the bulk density of the sorbents increased from 0.34 ± 0.06 cm^3/g to 0,95 ± 0.10. This indicates a decrease in the degree of porosity in them .

Adsorption experiments

The isotherms obtained from the sorption of benzene vapors on nanocomposite sorbents prepared in various solution media at 30°C were found to belong to type I according to the IUPAC classification (Figure 1).

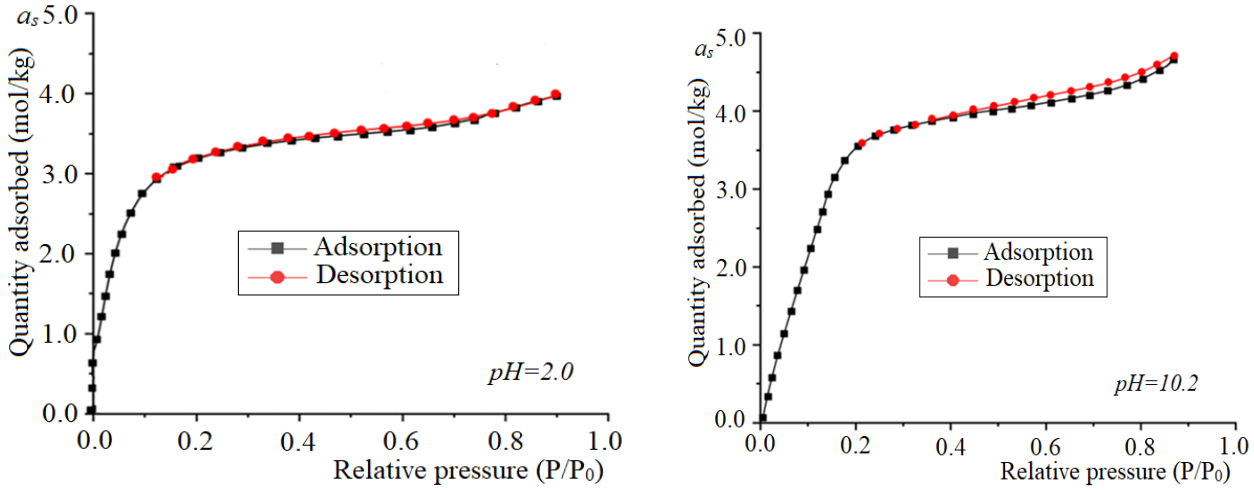

Figure 1. Benzene vapor sorption isotherms in the sorbents prepared in various -solution medium at 30°C

From the sorption isotherms, it can be seen that the relative pressure rises sharply from zero to p/p_s = 0,2 and saturates at p/p_s = 0,9 due to adsorbed benzene vapors. The degree of conformity of the graph 1 / a = f (1 / P) based on adsorbed benzene vapors at different relative pressures to the Lengmuir linear equation was found to be R^2 = 0,9812 (Figure 2). From the values obtained from the sorption of benzene vapors, the adsorption constant of Langmuir was calculated on the basis of the following linear equation.

$$\frac{p}{A} = \frac{1}{KA_\infty} + \frac{1}{A_\infty} \cdot p$$

According to the results of the calculations, it was found that the average value of Langmuir's adsorption constant is *K*=0,0362 .

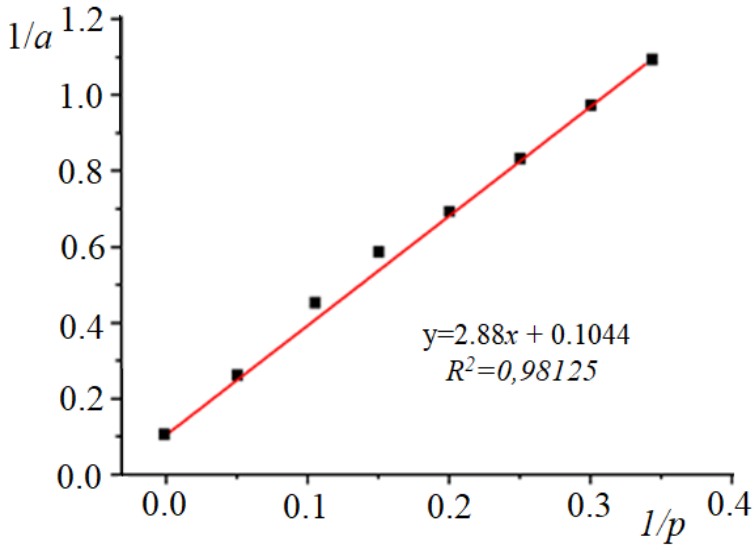

Figure 2. Conformity of the graph (1/*a* = *f* (1/P)) of benzene vapor sorption to the Langmuir linear equation

The average diameter of the sorbent pores synthesized at 30°C and their surface distribution were also studied using SEM analysis, and it was determined that the obtained results correspond to the values calculated using the BET equation (Figure 3).

From the figure, it can be seen that the surface of the sorbent $SiO_2 \cdot 0{,}3ZrO_2$ prepared in an acidic medium is monodespersed and it consists of spherically shaped particles. It was also found that the pores on the sorbent surface were uniform in size and that they were evenly distributed on the surface (Fig. 3a). The SEM image of the sorbent sample prepared in an alkaline medium revealed that its surface consisted of relatively larger pores (Fig. 3b).

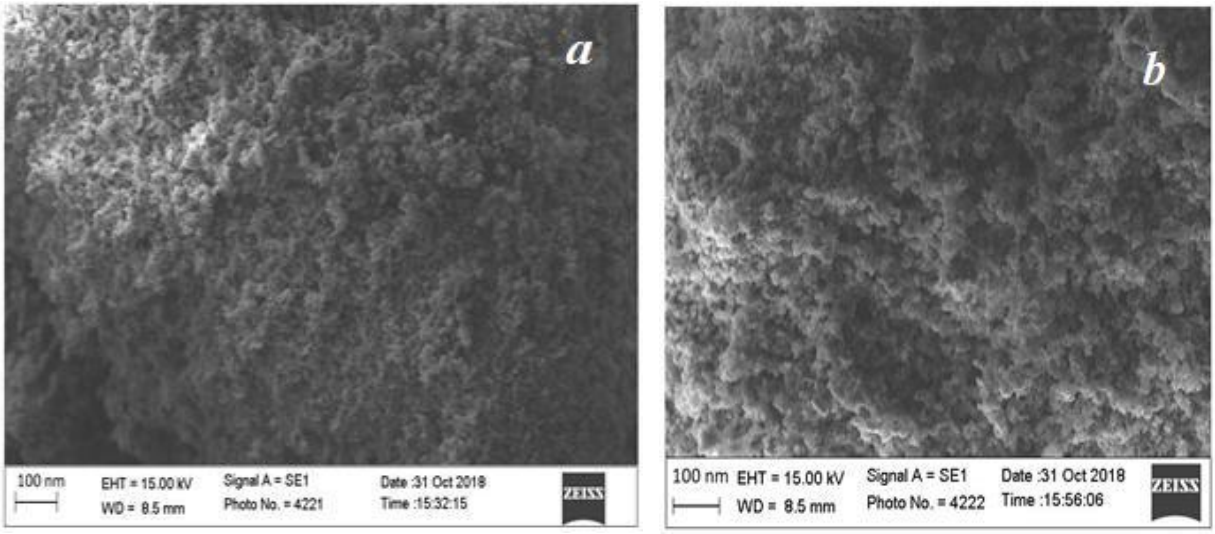

Figure 3. SEM image of the surface of the sorbents synthesized at 30°C and different solution medium (a) pH=2,0; b) pH=10,2)

Based on the results obtained in sorption isotherms and SEM, the specific surface area of the sorbents (S_{BET}, m^2/g), the average diameter of the pores (D, nm), monolayer capacity of the sorbents (a_m, mol/kg) and saturation adsorption (a_s, mol/kg) were calculated (Table 2).

Table 2

Texture characteristics of $SiO_2 \cdot 0{,}3ZrO_2$ nanocomposite sorbents prepared at 30°C and at different pH values

Adsorbent	pH	S_{BET}, m^2/g	a_m, mol/g	a_s, mol/g	D, nm
$SiO_2 \cdot 0{,}3ZrO_2$	2,0	975,6±100	2,6±0,02	6,2±0,08	0,8±0,05
	5,2	780,2±100	1,2±0,01	3,7±0,02	2,5±0,12
	10,2	710,3±100	0,85±0,06	3,1±0,02	2,8±0,06

It can be seen from the table, that the size of the pores changes with increasing solution pH in $SiO_2 \cdot 0{,}3ZrO_2$ sorbents synthesized at 30°C. The average pore diameter of the sorbent prepared at pH=2,0 was found to be 3,5 times smaller than the diameter of the sorbent pores prepared at pH=10,2 and the specific surface area was 1,37 times larger. It was also found that the saturation (a_s) of the composite sorbent synthesized in a strongly acidic medium on benzene vapor sorption was the highest, 1,67 times higher than that of the sorbent prepared at pH=5,2 and about 1,77 times higher than that of the sorbent prepared in a weakly alkaline medium.

As the size of the pores increased, a decrease in the amount of adsorbate adsorbed on the monolayer was observed. In the sorbent prepared in a strongly acidic medium, adsorption on the monolayer was found to be 41,91%, in the sorbent prepared at pH =5,2 - 32,43%, and in the sorbent synthesized in a weak alkaline medium - 27,42% (Table 3).

Table 3

Porosity by benzene vapor adsorption of SiO2 · 0.3ZrO2 nanocomposite sorbents synthesized at 30°C and at different pH values

pH	$W_0 \cdot 10^3$, cm^3/g	$W_{me} \cdot 10^3$, cm^3/g	$V_s \cdot 10^3$, cm^3/g
2,0	0,155 ± 0,04	0,224 ± 0,2	0,309 ± 0,25
5,2	0,216 ± 0,08	0,342± 0,1	0,558 ± 0,12
10,2	0,270± 0,04	0,416 ± 0,8	0,686 ± 0,15

It can be seen from the table, that the total porosity of the sorbent sample prepared in a weak alkaline medium is 0,270±0,04 cm^3/g, and the saturation volume is 1,23 times larger than that of the sorbent prepared in a weak acidic medium. This suggests that changes in the solution medium during synthesis have a direct effect on the volume of sorbent pores.

The sorption isotherms formed by the adsorption of benzene, hexane and toluene vapors on $SiO_2 \cdot 0{,}3ZrO_2$ nanocomposite sorbents synthesized at 50°C and in different media (pH= 2,0; pH=10,2) are shown in Figure 4.

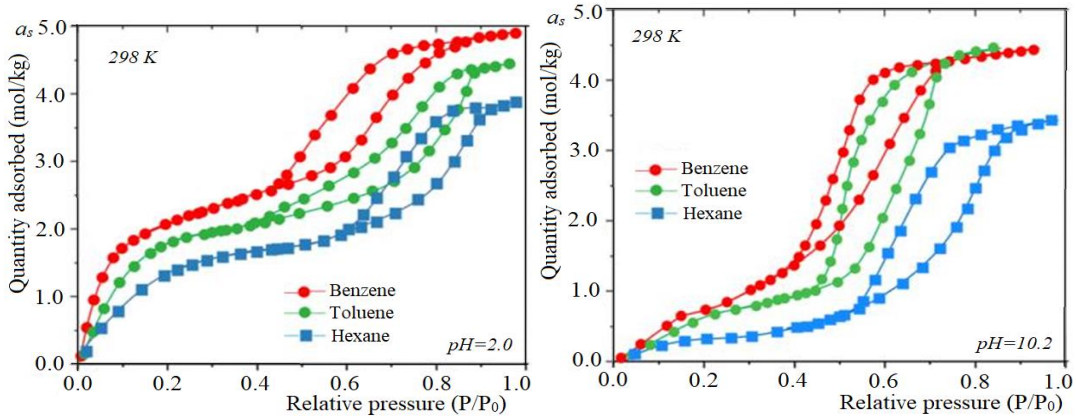

Figure 4. Sorption isotherms of VOC vapors on $SiO_2 \cdot 0{,}3ZrO_2$ sorbents prepared at 50°C and various solution medium

It was observed that the relative pressure at p/p_s=0,2 increased sharply and approached the saturation state at p/p_s=0,9 due to sorption of organic compounds vapors on the sorbent prepared at 50°C. It can be seen that the adsorption and desorption lines combine to form a hysteresis ring at p/p_s =0,4÷0,8 due to capillary condensation of the adsorbed vapors. It could be the basis for claiming that the sorbents prepared at 50°C consist of mesopores and the adsorption isotherm belongs to type IV according to the IUPAC classification.

The distribution of pores on the surface of $SiO_2 \cdot 0{,}3ZrO_2$ nanocomposite sorbents synthesized at 50°C and at 2,0 and 10,2 medium of the solution can be seen in Figure 5.

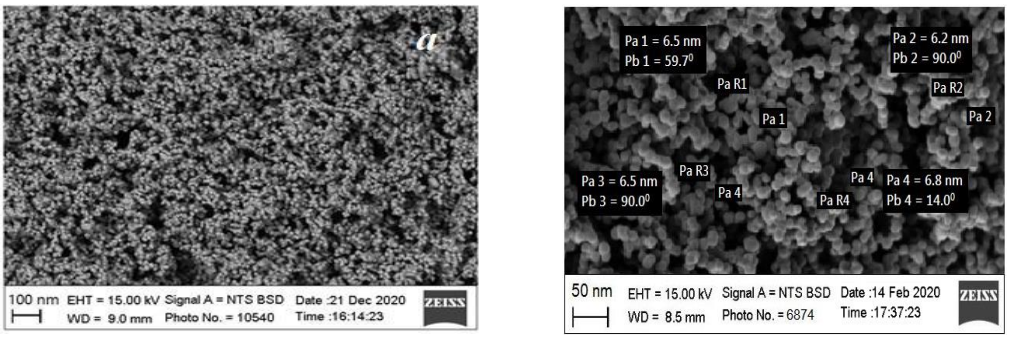

Figure 5. SEM image of the surface of sorbents prepared at 50°C at pH=2,0 (a) and pH = 10,2 (b)

It can be seen from the image that the sorbent pores prepared in an acidic medium are evenly distributed on the surface and are the same in size, while the surface of the sorbents prepared in an alkaline medium consists of monodispersed spherical morphological nanoparticles. The values for surface distribution of the pores on the sorbent samples synthesized at 50°C according to adsorption isotherms and the results obtained by SEM are given in Table 4. Also, based on the results obtained by SEM, the size distribution of pores on the surface of the sorbents was determined.

Table 4

Texture characteristics of $SiO_2 \cdot 0{,}3ZrO_2$ sorbents synthesized at 50°C

Sorbent	pH	S_{BET}, m^2/g	a_m, mol/kg	a_s, mol/kg	D, nm
$SiO_2 \cdot 0{,}3ZrO_2$	2,0	870,9±70,2	2,19 ± 0,18	6,2 ± 0,5	2,8 ± 0,25
	5,2	800,2±62,8	1,54 ± 0,11	4,3 ± 0,4	10,2 ± 0,92
	10,2	750,4±56,9	0,94 ± 0,07	3,8 ± 0,3	6,5± 0,42

It can be seen from the table that 35,4% of the amount of benzene adsorbed on the sorbent $SiO_2 \cdot 0{,}3ZrO_2$ prepared at pH=2,0, 35,8% on the sorbent prepared using CH_3COOH (pH=5,2) as a hydrolysis catalyst, 24.7% on the sorbent prepared using NH_4OH (pH=10,2) as a catalyst was found to be adsorbed on the monolayer.

According to that, 95,6-98,4% of the total pores in the sorbents correspond to mesopores and 5,3-1,6% to micropores (Figure 6).

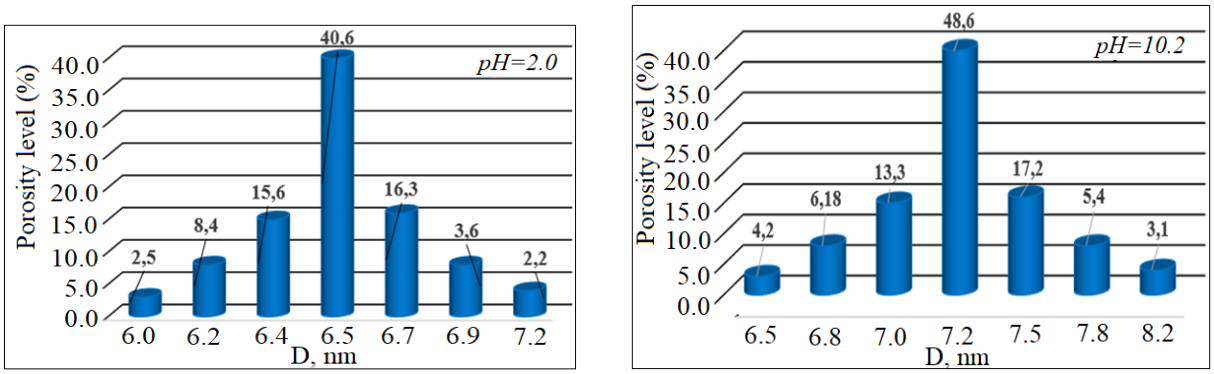

Figure 6. Size distribution of the pores on the surface of sorbents synthesized at pH 2,0 and 10,2 at 50°C

Also, based on the experimental data, the saturation volumes of the sorbents, the volume of the micropores (W_0), the volume of the mesopores (W_{mes}) and the saturation volume (V_s) on benzene vapors were determined (Table 5).

Table 5

Pore volumes of $SiO_2 \cdot 0{,}3ZrO_2$ nanocomposite sorbents synthesized at 50°C and different pH values

pH	$W_0 \cdot 10^3$, cm^3/g	$W_{me} \cdot 10^3$, cm^3/g	$V_s \cdot 10^3$, cm^3/g
2,0	0,324 ± 0,05	1,052 ± 0,06	1,376 ± 0,10
5,2	0,302 ± 0,01	0,911± 0,04	1.213 ± 0,24
10,2	0,182 ± 0,04	0,872 ± 0,08	1,054 ± 0,15

It can be seen from the table that the volume of the nanocomposite sorbent mesopores prepared under acidic conditions increased by 1,2 times compared to the volume of the sorbent pores prepared in weak alkaline medium, and the saturation volume increased by 1,3 times.

The sorption isotherms obtained from benzene vapor adsorption on the sorbents synthesized at 70°C and 90°C have shown that they consist of larger mesopores (Fig. 7).

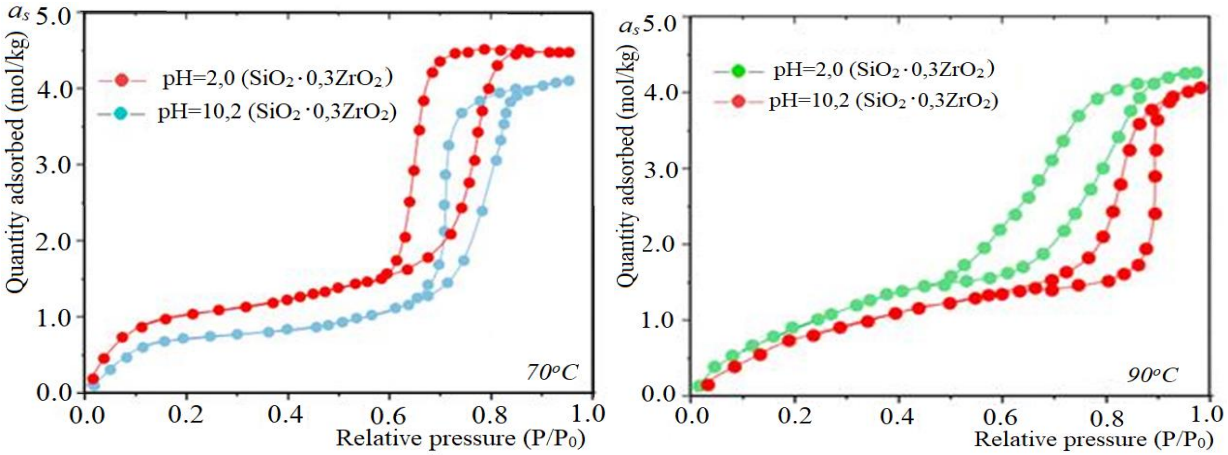

Figure 7. Benzene vapor sorption isotherms on $SiO_2 \cdot 0,3ZrO_2$ sorbents synthesized at 70°C and 90°C

It can be seen from the image that the hysteresis rings formed due to capillary condensation are enlarged in size and they shift towards a greater relative pressure

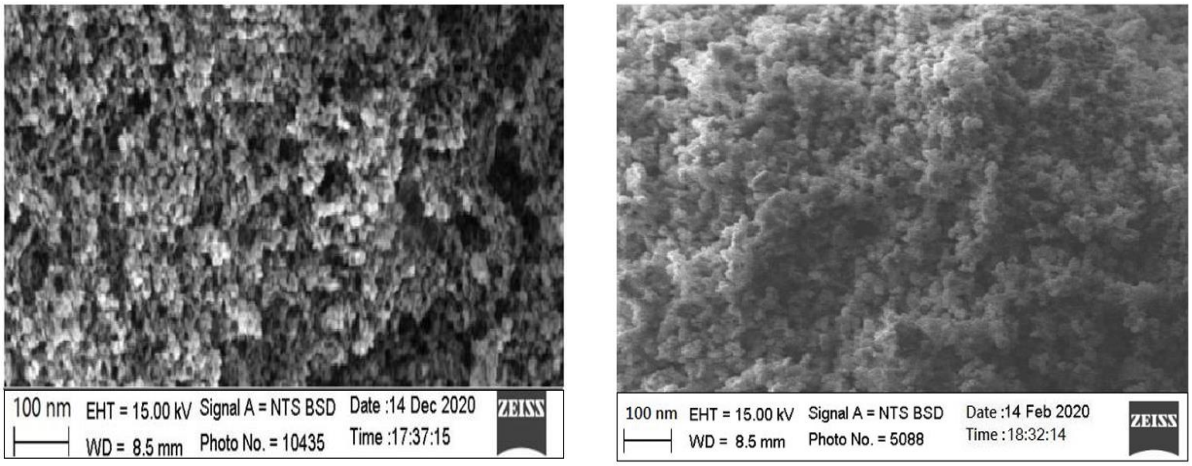

Figure 8. SEM image of the surface of the sorbents prepared at 70°C (a) and 90°C (b)

It was observed that the hysteresis rings in the samples prepared at 70°C are formed in interval of the relative pressure p/p_s=0,6÷0,9; and on the sorbents synthesized at 90°C in interval of p/p_s=0,65÷0,95.

It can be seen from the SEM image that the pores of $SiO_2 \cdot 0,3ZrO_2$ nanocomposite sorbents prepared at 70°C and 90°C consist of large mesopores.

Table 6

Texture characteristics of $SiO_2 \cdot 0,3ZrO_2$ nanocomposite sorbents prepared at different temperatures

t°C	pH	S_{BET}, m^2/g	a_s, mol/kg	D, nm
70	2,0	450,8 ± 35,0	3,5 ± 0,3	25,3±2,2
	5,2	456,2± 36,1	3,2 ± 0,3	25,2± 2,1
	10,2	436,2±34,8	2,8 ± 0,2	48,6 ± 3,8
90	2,0	400,3±32,6	1,6 ± 0,1	52,2 ± 4,8
	5,2	350,6±29,8	1,6 ± 0,1	60,5 ±5,2
	10,2	356,5±30,2	0,8 ± 0,1	72,8 ±6,4

The pores on the sorbent synthesized at 120°C were found to correspond to macropores (Fig. 9).

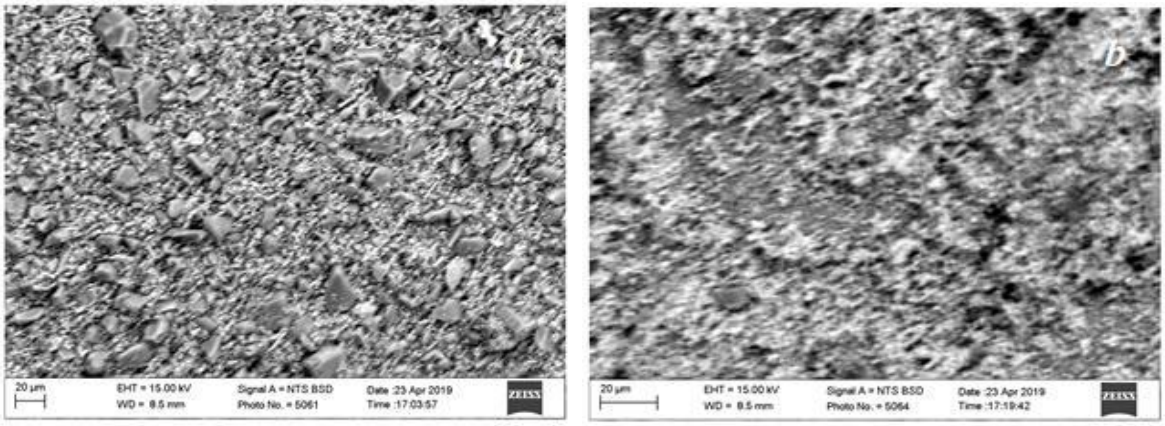

Figure 9. SEM images of the sorbents prepared in acidic (a) and alkaline media (b) at 120°C

It can be seen from the image that the pores are unevenly distributed on the surface of the sorbents prepared in different solution medium at 120°C and they correspond in size to the macro pores.

The benzene vapor adsorption isotherms of the sorbent samples synthesized at 50°C, 70° C, and 90°C were found to conform to the linear form of the BET equation. $\frac{p/p_s}{a(1-p/p_s)} = \frac{1}{a_m \cdot C} + \frac{C-1}{a_m \cdot C} \cdot (p/p_s)$

Dependence graph of the adsorbed amount of the adsorbate on different values of the relative pressure has been reated (Fig.10)

It was also found that the formation of the structure and size of the pores during the synthesis depending on the solution medium determines the sorption capacity of the adsorbents. The increase in temperature during the sol-gel process has a direct effect on the degree of porosity of the sorbents. Based on the above data, it can be concluded that the adsorption capacity of the sorbents prepared at relatively low temperatures for various organic compounds is high (Fig. 10-*b*).

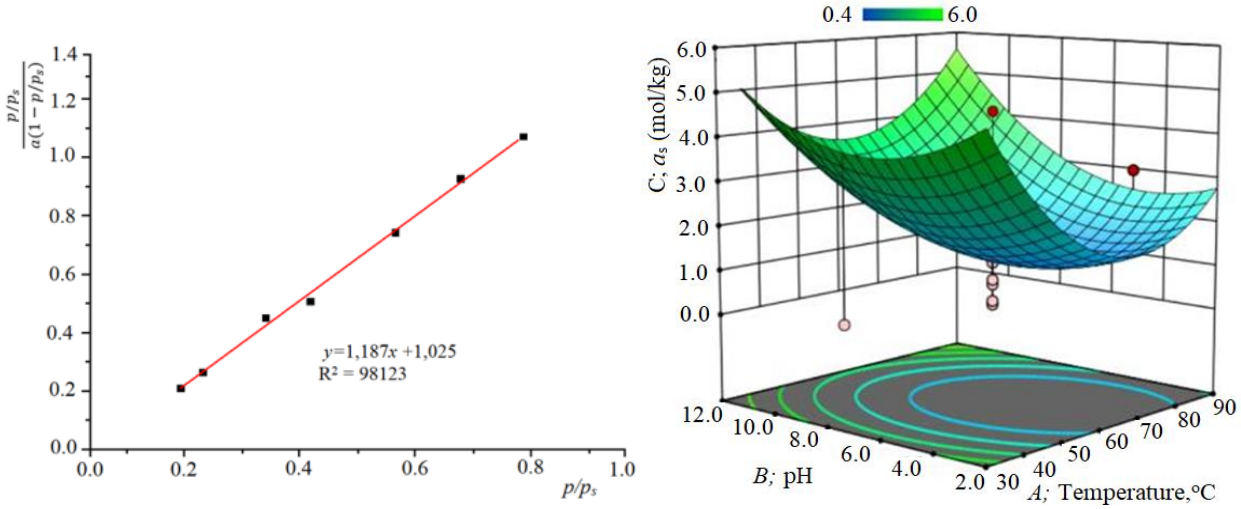

Figure 10. Correspondence of the values of benzene vapor sorption on the mesopores to the linear BET equation (*b*) and changes in the sorption capacity (*a*)

In sector A of the figure, a decrease in sorption capacity of the sorbents (a_s, sector C) was observed with increasing temperature. It can be seen from sector B that the sorption capacity of the nanocomposite sorbents prepared in a strongly acidic medium is high, a slight decrease in this

value was observed, when it was converted to a weakly acidic medium. In the sorbents prepared in a weak alkaline medium in the presence of ammonia as a catalyst for hydrolysis, an increase in sorption capacity was observed. In general, the effect of solution medium (pH) and temperature on the specific surface area and porosity of the sorbents during the synthesis can be seen from the following 3D graphs (Figure 12).

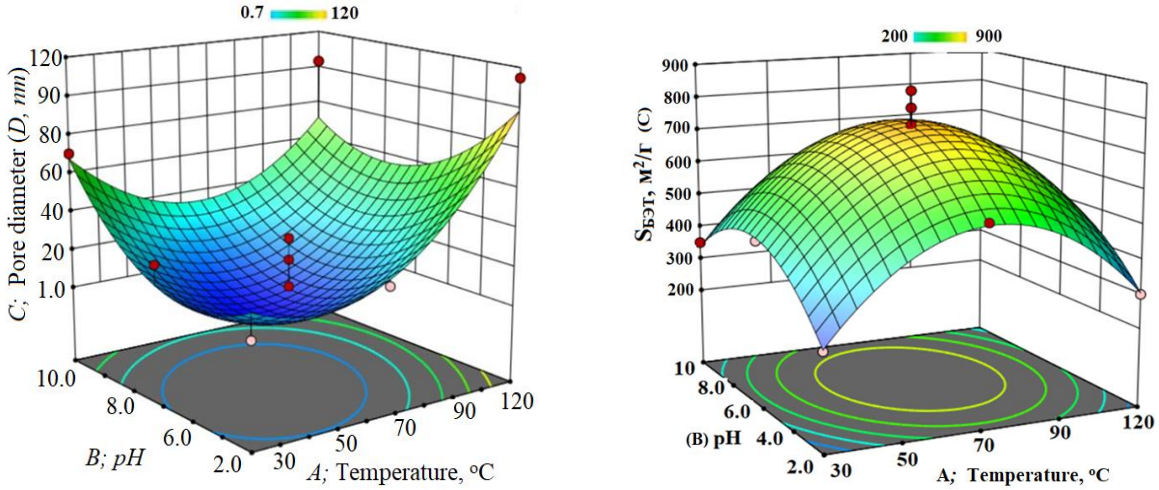

Figure 12. The effect of solution medium and temperature on the formation of pores size (*a*) and specific surface (*b*) of the sorbents.

As it can be seen from the figure, the change in pore size is linearly depended on the increase in the temperature. It was found that an increase in temperature had a greater effect to the pore size than the increase in pH value of the solution.

The phase composition of $SiO_2 \cdot xZrO_2$ nanocomposite sorbent was studied by X-ray diffractometry method. An Empyrean, Malvern Panalytical (Germany) X-ray diffractometer (XRD) equipped with a modern computer was used to perform the X-ray analysis of the samples. The obtained diffractograms were analyzed by a semi-quantitative method using calibration standards (Fig.13).

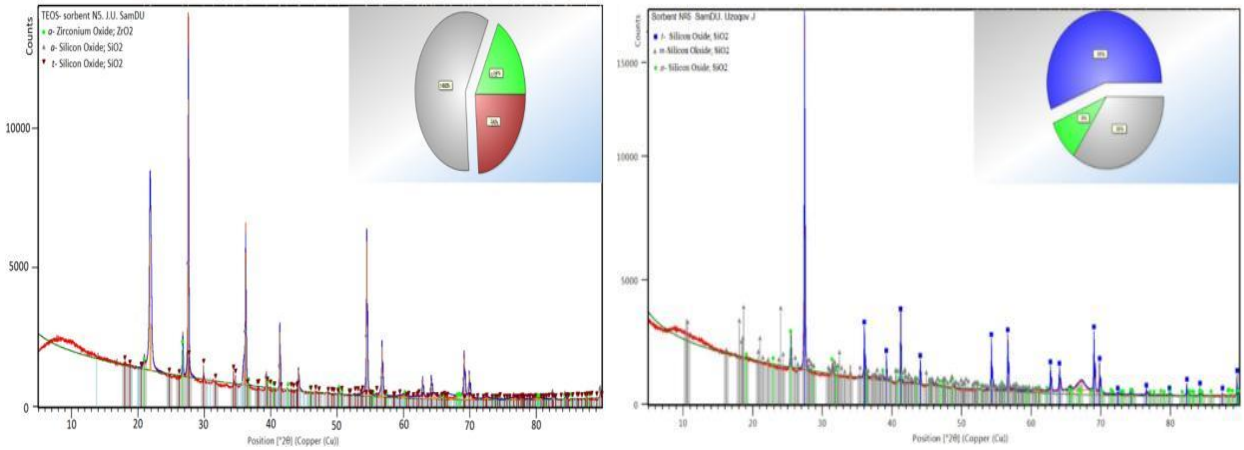

Figure 13. Phase composition of $SiO_2 \cdot 0{,}3ZrO_2$ nanocomposites sorbents

From the figure, it was observed that the areas 2θ = 18,1° - 82° consist of dense weak signal spectra of amorphous SiO_2. The formation of weak signal spectra of amorphous ZrO_2 were formed in the areas of 2θ = 20,4 °; 27,9 °; 36,5° and 69,2°; 82 °. The formation of high-intensity spectra of tetrahedral SiO_2 was determined in 2θ = 22,8°; 28.2°; 36,4°; 55,6°; 57,2°. The phase

composition of the sorbent was found to be 55.2% amorphous SiO_2, 6,5% tetrahedral SiO_2 and 38.3% amorphous ZrO_2. It corresponds exactly to the composition $SiO_2 \cdot 0{,}3ZrO_2$.

The EDS analysis of $SiO_2 \cdot xZrO_2$ nanocomposite sorbents synthesized at different temperatures also revealed that the element composition of the sorbent samples corresponded to the composition of the reagents [45].

It can be seen from the figure that the spectra of the electromagnetic emission radiation of O element can be observed in the 0,5 keV field. It was also observed that there are emission spectra formed by excited electrons in elements Si at 1,8 keV and Zr at 2,8 keV. The mass fraction (%) of the elements in the sorbent sample was found to be O-43,5 ± 3,2%, Si-28,2 ± 2,2% and Zr-28,3 ± 1,4% .

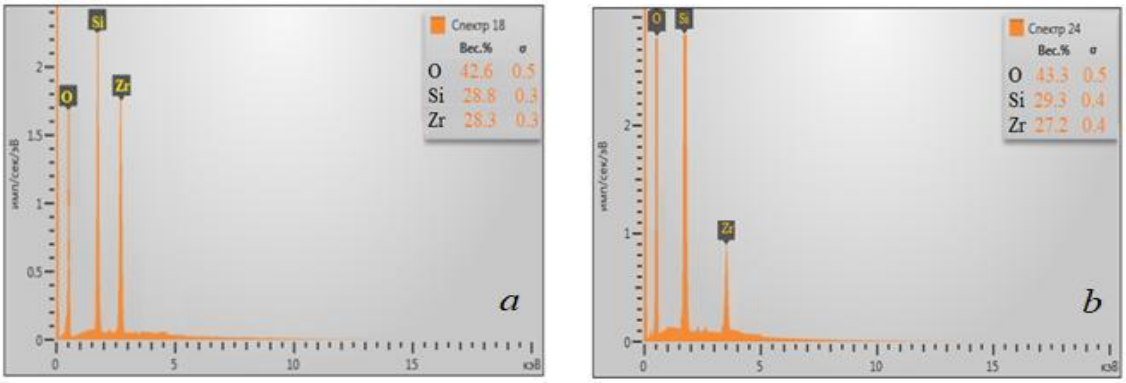

Figure 14. EDS analysis of $SiO_2 \cdot 0{,}3ZrO_2$ nanocomposites sorbents.

$SiO_2 \cdot xZrO_2$ (x =0,3 ÷ 0,7) nanocomposites sorbents were used to separate methylene blue dye in the wastewater of textile factories.The amount absorbed by methylene blue on the sorbent was found from the difference between the initial concentration of the dye (C_i) and the equilibrium concentration (C_e). The absorbed mass (g) of the dye on the sorbent was calculated using the following formula:

$$n = (C_i - C_a)V,$$

The specific sorption amount (qe) was calculated using the following formula:

$$q_e = \frac{n}{m_c}, \frac{mol}{g},$$

where n is the amount of sorbed methylene blue, mol; C_i initial concentration of dye solution, mol/l; C_a-concentration of the dye solution after sorption, mol/l; V is the volume of methylene blue solution (l); q_e- specific sorption amount, mol/g; m_c- sorbent mass, (g).

The adsorption efficiency of methylene blue dye on the sorbents of different composition can be seen in figure 15.

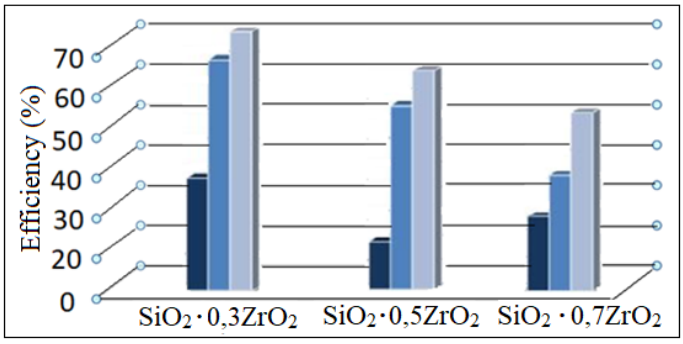

Figure 15. The adsorption efficiency of methylene blue on the sorbents.

4. Conclusions

$SiO_2 \cdot xZrO_2$ (x = 0,3; 0,5; 0,7) composite sorbents were synthesized using the sol-gel technology. The effect of temperature, solution medium and reagent concentration on the texture characteristics of the sorbents, including the specific surface area, the average diameter and volume of the pores was studied. According to that it was determined that the average diameter of the pores is D = 2,5 ÷ 32,1 nm, the surface area is S_{BET} = 200 ÷ 975,6 m^2/g, the average volume of the pores is V_s = 0,205 ÷ 0,412 cm^3/g for the sorbents prepared in different solution media and temperatures. It was noted that sorption isotherms obtained from the adsorption of organic substances on the sorbents containing $SiO_2 \cdot xZrO_2$ were studied. The isotherms obtained at 30°C were classified as type I and the isotherms obtained at 50°C, 70°C and 90°C as type IV according to IUPAC classification.

REFERENCES

1. Baig N., Kammakakam I., Falath W. Nanomaterials: A review of synthesis methods, properties, recent progress, and challenges //Materials Advances. – 2021. – T. 2. – №. 6. – C. 1821-1871.
2. Uzokov J. R., Mukhamadiev N. K. Sorption characteristics of the mesoporous sorbents based on tetraethoxysilane and titanium oxide //European Journal of Molecular & Clinical Medicine. – 2020.– T. 7. – №. 07. – C. 656-660.
3. Xu M. et al. How entanglement of different physicochemical properties complicates the prediction of in vitro and in vivo interactions of gold nanoparticles //ACS nano. – 2018. – T. 12. – №. 10. – C. 10104-10113.
4. Uzokov J. R., Mukhamadiev N. K. Sorption characteristics of mesoporous composite $SiO_2 \cdot TiO_2$ //Central Asian Journal of Medical and Natural Science. – 2021. – T. 2. – №. 5. – C. 494-498.
5. Diyarov A. A. Mukhamadiev, N. Q., Uzokov, J. R.Synthesis of mesoporous sorbents on the basis of Al2O3 and their textural characteristics //Central Asian Journal of Medical and Natural Science. – 2022. – T. 3. – №. 3. – C. 511-518.
6. Usmonova H. Uzokov, J. R., Mukhamadiev, N. Q.,Study of structural and electronic properties of (ZnO) n (n= 10÷ 30) nanoclusters using quantum chemical methods //central asian journal of medical and natural science. – 2022. – T. 3. – №. 6. – C. 428-434.
7. Arzimurodova X. Ismatov, D. M., Uzokov, J. R., Mukhamadiyev, A. N., Mukhamadiev, N. Q.Quantum chemical evaluation of complex formation of Co (II) ions with quercetin molecule //Central Asian Journal of Medical and Natural Science. – 2022. – T. 3. – №. 3. – C. 338-344.
8. Mamaziyaeva S. Uzokov, J. R., Mukhammadiyev, N. Q., Synthesis and their texture characteristics of mesoporous silica gel as surfactant supporting rutin //Central Asian Journal of Medical and Natural Science. – 2023. – T. 4. – №. 2. – C. 608-614.
9. Ulugboyeva G. O., Uzokov, J. R., Mukhammadiyev, N. Q., & Mukhamadiyev, A. N. Amorphous silica gel as a surfactant for saponins: support, synthesis, and texture characteristics //Central Asian Journal of Medical and Natural Science. – 2023. – T. 4. – №. 2. – C. 601-607.
10. Husenov F. N. Uzokov, J. R., Mukhammadiyev, N. Q., Tashmatova, R. V., & Mukhamadiyev, A. N. Synthesis of mesoporous AL2O3 and study of its sorption properties //Central Asian Journal of Medical and Natural Science. – 2023. – T. 4. – №. 2. – C. 596-600.

11. Сайиткулов Ш. М. Узоков, Ж., Саидов, Х. М., & Мухамадиев, Н. К. Изучение текстурных характеристик оксида кремния как носителя катализаторов //XXXV Всероссийский симпозиум молодых ученых по химической кинетике. – 2018. – С. 124-124.
12. Soltani R, Marjani A, Soltani R, Shirazian S (2020) Hierarchical multi-shell hollow micro–meso–macroporous silica for Cr (VI) adsorption. *Scientific reports 10*(1):1-12.
13. Zhu C, Du D, Eychmüller A, Lin Y (2015) Engineering ordered and nonordered porous noble metal nanostructures: synthesis, assembly, and their applications in electrochemistry. Chemical reviews *115*(16):8896-8943.
14. Yamashita H, Mori K, Kuwahara Y, Kamegawa T, Wen M, Verma P, Che z (2018) Single-site and nano-confined photocatalysts designed in porous materials for environmental uses and solar fuels. Chemical Society Reviews *47*(22):8072-8096.
15. Souza J, Oliveira G, Alexandre J, Neto J, Sales M, Junior P, Santos J (2022) A comprehensive review on the use of metal–organic frameworks (MOFs) coupled with enzymes as biosensors. *Electrochem 3*(1):89-113.
16. Alswat AA, Ahmad MB, Saleh TA (2017) Preparation and characterization of zeolite\zinc oxide-copper oxide nanocomposite: antibacterial activities. Coll Interface Sci Comm 16:19–24. https://doi.org/10.1016/j.colcom.2016.12.003
17. Collins MN, Nechifor M, Tanasă F, Zănoagă M, McLoughlin A, Stróżyk MA, Teacă CA (2019) Valorization of lignin in polymer and composite systems for advanced engineering applications–a review. International journal of biological macromolecules *131*:828-849.
18. Diaconu A, Chiriac A, Neamtu, Nita L, (2019). Magnetic polymeric nanocomposites. Polymeric nanomaterials in nanotherapeutics 359-386.
19. Xu W, He W, Du Z, Zhu L, Huang K, Lu Y, Luo Y (2021) Functional nucleic acid nanomaterials: Development, properties, and applications. Angewandte Chemie International Edition 60(13):6890-6918.
20. Wongkaew N, Simsek M, Griesche C, Baeumner AJ (2018) Functional nanomaterials and nanostructures enhancing electrochemical biosensors and lab-on-a-chip performances: recent progress, applications, and future perspective. Chemical reviews 119(1):120-194.
21. Zhai Y, Dou Y, Zhao D, Fulvio PF, Mayes RT, Dai S (2011) Carbon materials for chemical capacitive energy storage. *Advanced materials 23*(42):4828-4850.
22. Tielas A, etc (2014) Nanomaterials - Guide for the SUDOE space industry. Portugal
23. Alves AK (2021) Technological Applications of Nanomaterials. Switzerland AG
24. Putzbach W, Ronkainen NJ (2013) Immobilization techniques in the fabrication of nanomaterial-based electrochemical biosensors: A review. *Sensors 13*(4):4811-4840.
25. Bardestani, R., Patience, G. S., Kaliaguine, S. (2019). Experimental methods in chemical engineering: specific surface area and pore size distribution measurements—BET, BJH, and DFT. The Canadian Journal of Chemical Engineering, 97(11), 2781-2791.
26. Kao, K. C., Mou, C. Y. (2013). Pore-expanded mesoporous silica nanoparticles with alkanes/ethanol as pore expanding agent. Microporous and mesoporous materials, 169, 7-15.
27. Issa, A. A., Luyt, A. S. (2019). Kinetics of alkoxysilanes and organoalkoxysilanes polymerization: a review. Polymers, *11*(3), 537.

28. Ying, J. Y., Mehnert, C. P., Wong, M. S. (1999). Synthesis and applications of supramolecular-templated mesoporous materials. Angewandte Chemie International Edition, *38*(1-2), 56-77.
29. Cherrak R, Hadjel M, Benderdouche N, Adjdir M, Mokhtar A, Khaldi K, Weidler P (2020). Preparation of nano-TiO_2/diatomite composites by non-hydrolytic sol–gel process and its application in photocatalytic degradation of crystal violet. Silicon 12(4):927-935.
30. Huang G, Li W, & Song Y (2018) Preparation of SiO_2–ZrO_2 xerogel and its application for the removal of organic dye. Journal of Sol-Gel Science and Technology 86(1):175-186. https://doi.org/10.1007/s10971-018-4611-4
31. Uzokov JR, Mukhamadiev NK (2021) Synthesis of mesopore $SiO_2 \cdot xZrO_2$ nanocomposite sorbents and their texture characteristics. Scientific bulletin of Samarkand State University Special Issue:32-33.
32. Uzokov JR, Muhamadiyev NK (2019) Synthesis of nanosorbents for chromatography from tetraethoxysilane and metal oxides. Proceedings of the International scientific-practical conference “Achievements, problems and prospects of complex innovative development of the Zarafshan oasis” (pp.366-368). Navoiy.
33. Uzokov JR, Mukhamadiev NK (2021) Sorption characteristics of mesoporous composite $SiO_2 \cdot TiO_2$. Central Asian journal of Medical and Natural sciences *2*(5):494-498.
34. Uzokov JR, Mukhamadiev NK, Sayitkulov ShM (2018) Study of the texture characteristics of silicon oxide as a carrier of catalysts. Book of abstracts of the XXXV All-Russian Symposium of Young Scientists on Chemical Kinetics. (p.162). Moscow. (in Russian).
35. Uzokov JR, Mukhamadiev NK (2020) Sorption characteristics of mesoporous sorbents based on tetraethoxysilane and titanium dioxide. Book of abstracts of Open school-conference of the CIS countries "Ultra fine grain and nanostructural materials» (pp. 400-402) Ufa, Russia (in Russian).